

loss of crystallinity that occurs at 200 K (a temperature at which the compound is stable) may correspond to mechanical destruction of the crystals, leading to a severe mosaic spread and tending toward amorphous character.

Single-crystal data at or near 200 K for $\text{Rb}^+(15\text{C}_5)_2\text{Na}^-$, $\text{Rb}^+(15\text{C}_5)_2\text{Rb}^-$, and $\text{Cs}^+(15\text{C}_5)_2\text{K}^-$ (monoclinic, $C2/m$) were used to simulate the X-ray powder patterns. A good match of the peak positions allowed us to index the diffraction peaks and showed that the powder samples were monophasic. This is important, since single crystals for structure determination can often be picked from a mixture that contains other compounds or structural types.

The refinement of the X-ray powder pattern for these three known compounds at 200 K gives the data in Table I. For $\text{Rb}^+(15\text{C}_5)_2\text{Na}^-$ and $\text{Rb}^+(15\text{C}_5)_2\text{Rb}^-$, the data at 80 K are also included. Only a small change in the cell parameters occurs as the temperature is decreased from 200 to 80 K.

The two compounds of unknown structure, $\text{K}^+(15\text{C}_5)_2\text{K}^-$ and $\text{K}^+(15\text{C}_5)_2\text{Na}^-$, had powder patterns sufficiently similar to those of known structure to permit refinement, although complications resulted from the phase transition observed for these two compounds.

The XRD powder pattern of $\text{K}^+(15\text{C}_5)_2\text{Na}^-$ at 80 K is very similar to that of $\text{Rb}^+(15\text{C}_5)_2\text{Na}^-$, so that refinement of the cell parameters of the former compound could be readily made by starting with structural data for the latter compound. However, the phase transition that occurred between 80 and 200 K yielded a new pattern that did not permit refinement and may have resulted from a mixture. Therefore, Table I contains cell parameters for $\text{K}^+(15\text{C}_5)_2\text{Na}^-$ only at 80 K.

Interestingly, the powder pattern of $\text{K}^+(15\text{C}_5)_2\text{K}^-$ at 200 K is similar to that of $\text{Rb}^+(15\text{C}_5)_2\text{Na}^-$ at 80 K, permitting refinement at 200 K. The pattern at 80 K for the former compound is sufficiently different that refinement was not possible.

Both $\text{Cs}^+(15\text{C}_5)_2\text{Na}^-$ and $\text{Cs}^+(15\text{C}_5)_2\text{e}^-$ are triclinic ($P\bar{1}$).^{10,17} In each case, one of the $-\text{CH}_2-$ groups is disordered and the single-crystal data were refined by using half-occupancy for each site. The program used for the simulation of powder patterns does not allow inclusion of partial occupancy. Nevertheless, the simulated powder patterns obtained by ignoring the disorder agreed well with the observed patterns. Because of missing low-angle diffraction peaks, however, it was not possible to refine the powder diffraction data.

The XRD powder patterns of $\text{Rb}^+(15\text{C}_5)_2\text{e}^-$ and $\text{K}^+(15\text{C}_5)_2\text{e}^-$ were also obtained. However, severe broadening of the diffraction peaks of the latter and the very low intensity at low angles of the former made the study difficult. Also, it is difficult in the synthesis of $\text{Rb}^+(15\text{C}_5)_2\text{e}^-$ and $\text{K}^+(15\text{C}_5)_2\text{e}^-$ to avoid formation of mixtures with the corresponding alkali. It appears from the diffraction data that $\text{Rb}^+(15\text{C}_5)_2\text{e}^-$ belongs to the monoclinic system. The data for $\text{K}^+(15\text{C}_5)_2\text{e}^-$ were not good enough to permit assignment of the crystal system.

Summary

From these results several points can be made: (1) The two sodides $\text{K}^+(15\text{C}_5)_2\text{Na}^-$ and $\text{Rb}^+(15\text{C}_5)_2\text{Na}^-$, the two potassides $\text{Cs}^+(15\text{C}_5)_2\text{K}^-$ and $\text{K}^+(15\text{C}_5)_2\text{K}^-$, and the rubidide $\text{Rb}^+(15\text{C}_5)_2\text{Rb}^-$ all belong to the monoclinic system and are probably isostructural. (2) For $\text{Cs}^+(15\text{C}_5)_2\text{Na}^-$, $\text{Cs}^+(15\text{C}_5)_2\text{K}^-$, $\text{Rb}^+(15\text{C}_5)_2\text{Na}^-$, $\text{Rb}^+(15\text{C}_5)_2\text{Rb}^-$, and $\text{Cs}^+(15\text{C}_5)_2\text{e}^-$, from 80 to 200 K a shift of the diffraction peaks to low angle is observed that corresponds to a slight change of the cell parameters. This is reversible except in the case of $\text{Cs}^+(15\text{C}_5)_2\text{e}^-$. (3) For $\text{K}^+(15\text{C}_5)_2\text{Na}^-$ and $\text{K}^+(15\text{C}_5)_2\text{K}^-$, a phase transition occurs between 80 and 200 K.

The determination of the cell parameters from X-ray powder diffraction data for compounds for which it has been impossible to obtain single crystals can be accomplished for alkaliides and electrides when a comparison with similar known compounds is

possible. By indexing the diffractograms of known compounds, it is possible to index those of the unknown compounds and to refine the cell parameters. However, to do this, XRD powder patterns of high quality are required and it is not always possible to obtain such data for alkaliide and electride compounds.

This technique will prove useful to assess the purity and detect any phase transitions that might occur for these compounds. Temperature studies can give information about thermal motions of the atoms, especially those of the complexant.

Acknowledgment. This research was supported in part by National Science Foundation Solid-State Chemistry Grant DMR 87-14751. We are grateful to the Michigan State University Center for Fundamental Materials Research for providing funds for equipment and for partial support for K.-L.T.

Supplementary Material Available: Diffractograms and tables of peak positions, d spacings, integrated intensities, peak heights, and half-widths for all compounds studied (44 pages). Ordering information is given on any current masthead page.

Contribution No. 8155 from the Arnold and Mabel Beckman Laboratories of Chemical Synthesis, California Institute of Technology, Pasadena, California 91125

Structure of Disodium *trans*-Bis(2,6-pyridinedicarboxylato-*O,N*)platinate(II) Hexahydrate

A. M. Herring, L. Henling, J. A. Labinger,* and J. E. Bercaw*

Received June 19, 1990

As part of our studies on alkane activation by aqueous platinum(II) complexes,¹ we have sought to prepare square-planar chelate platinum complexes where all the ligating atoms are *hard*. Our first test case was the known² $[\text{Pt}(\text{dipic})\text{Cl}]^-$, where *dipic* = 2,6-pyridinedicarboxylate; this compound in fact does not effect alkane activation, possibly because the pyridine ligand is too soft. In the course of the preparation large crystals of a different complex were obtained; this product appeared to be the same as a secondary product observed by Kostic and was assigned as *trans*- $[\text{Pt}(\eta^2\text{-dipic-}O,N)_2]^{2-}$ on the basis of its NMR spectrum.² Structures of complexes containing *dipic* as a *bidentate* ligand are quite rare—only that of the *protonated* $[\text{RuCl}_2(\eta^2\text{-dipicH-}O,N)_2]^-$ has been reported³—and structural assignments based only upon NMR spectra for related chelates of platinum⁴ have proven to be incorrect;⁵ hence, we felt it worthwhile to carry out a crystallographic structure determination.

Experimental Section

Synthesis. A mixture of 0.22 g (1.04 mmol) of disodium 2,6-pyridinedicarboxylate (prepared by neutralizing commercial 2,6-pyridinedicarboxylic acid with NaOH) and 0.20 g (0.52 mmol) of Na_2PtCl_4 (Aesar) in 2 mL of H_2O was stirred under Ar until all solids dissolved and allowed to stand; after 24 h a mixture of yellow prisms and purple needles (0.24 g total) was filtered off. The yellow prisms were separated by hand and recrystallized from H_2O .

¹H NMR (D_2O): δ 8.14, t; δ 7.72, dd; δ 7.53, dd; $^3J_{\text{HH}} = 7.5$ Hz; $^4J_{\text{HH}} = 1.5$ Hz. IR (cm^{-1} , Nujol): 3600 w, 3501 w, 2405 m, 2396 m, 1624 s, 1459 m, 1416 m, 1265 m, 1211 w, 1140 w, 1097 w, 1038 w, 916 w. The elemental analysis agreed best with a dihydrate formula, not the hexahydrate determined crystallographically, presumably indicating partial dehydration in handling; it was necessary to protect the crystals

(1) Labinger, J. A.; Herring, A. M.; Bercaw, J. E. *J. Am. Chem. Soc.* **1990**, *112*, 5628.

(2) Zhou, X.-Y.; Kostic, N. M. *Inorg. Chem.* **1988**, *27*, 4402.

(3) Ventur, D.; Wieghardt, K. *Z. Anorg. Allg. Chem.* **1985**, *524*, 40.

(4) Smith, B. B.; Sawyer, D. T. *Inorg. Chem.* **1969**, *8*, 379.

(5) Appleton, T. G.; Berry, R. D.; Hall, J. R. *Inorg. Chem.* **1985**, *24*, 666.

(17) Ward, D. L.; Huang, R. H.; Kuchenmeister, M. E.; Dye, J. L. *Acta Crystallogr., Sect. C* **1990**, *C46*, 1831.

Table I. Crystallographic Data for Disodium *trans*-Bis(2,6-pyridinedicarboxylato-*O,N*)platinate(II) Hexahydrate

formula: PtC ₁₄ H ₁₈ O ₁₄ N ₂ Na ₂	fw: 679.36
<i>a</i> = 11.902 (5) Å	space group: <i>P</i> 2 ₁ / <i>c</i> (No. 14)
<i>b</i> = 6.538 (2) Å	λ = 0.7107 Å
<i>c</i> = 12.690 (7) Å	ρ_{calc} = 2.286 g cm ⁻³
β = 91.53 (2)°	μ = 76.11 cm ⁻¹
<i>V</i> = 987.1 (7) Å ³	transm coeff = 0.08–0.17
<i>Z</i> = 2	<i>R</i> (<i>F</i> _o) = 0.0250
<i>T</i> = 297 K	GOF = 1.96

Table II. Final Non-Hydrogen Coordinates and Displacement Parameters for Disodium *trans*-Bis(2,6-pyridinedicarboxylato-*O,N*)platinate(II) Hexahydrate (*x*, *y*, *z*, and *U*_{eq}^a × 10⁴)

atom	<i>x</i>	<i>y</i>	<i>z</i>	<i>U</i> _{eq} , Å ²
Pt	0	0	0	150 (0.5)
N	-424 (2)	691 (4)	1485 (1)	174 (4)
O1	1525 (1)	755 (3)	604 (1)	251 (4)
O2	2474 (1)	951 (3)	2136 (2)	318 (4)
O3	-2242 (1)	2901 (3)	526 (1)	290 (4)
O4	-3348 (2)	605 (4)	1288 (2)	361 (5)
C1	1591 (2)	763 (4)	1627 (2)	211 (4)
C2	483 (2)	670 (4)	2155 (2)	192 (4)
C3	381 (2)	684 (5)	3234 (2)	224 (5)
C4	-693 (2)	702 (5)	3641 (2)	243 (5)
C5	-1610 (3)	856 (4)	2957 (2)	234 (5)
C6	-1459 (2)	906 (4)	1873 (2)	185 (4)
C7	-2435 (2)	1488 (4)	1148 (2)	218 (5)
Na	-4178 (1)	-2629 (2)	1737 (1)	337 (2)
O5	-3410 (2)	-3610 (4)	61 (2)	364 (5)
O6	-5011 (2)	-1278 (4)	3327 (2)	367 (5)
O7	-5845 (2)	-1482 (5)	996 (3)	619 (8)

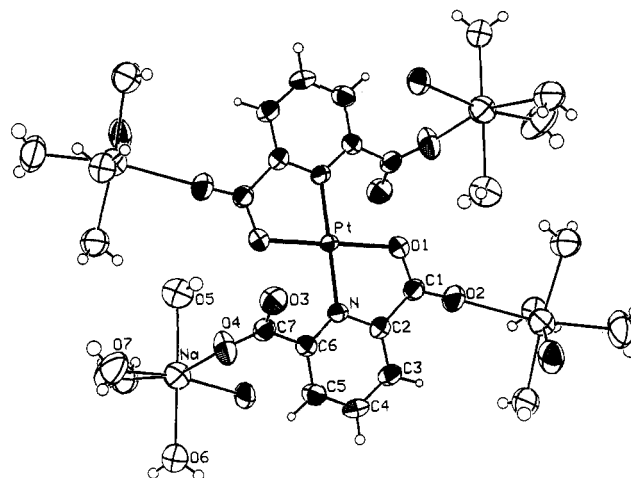
$$^a U_{\text{eq}} = \frac{1}{3} \sum_i \sum_j [U_{ij}(a_i^* a_j^*) (\bar{a}_i \bar{a}_j)]$$

against solvent loss during data acquisition. Anal. Calcd for C₁₄H₁₀N₂Na₂O₁₀Pt: C, 27.69; H, 1.66; N, 4.61. Found: C, 27.91; H, 1.36; N, 4.81.

Crystallography. A crystal was mounted on a glass fiber, coated with epoxy as a precaution against solvent loss, and centered on a CAD-4 diffractometer. Unit cell parameters and an orientation matrix were obtained by a least-squares calculation from the setting angles of 24 reflections with $14^\circ < 2\theta < 20^\circ$. Two equivalent data sets out to a 2θ of 60° were collected. The data were corrected for absorption and decay. An average background as a function of 2θ was calculated but not used. Lorentz and polarization factors were applied, and the two data sets were then merged to yield the final data set. Absences in the diffractometer data showed the space group to be *P*2₁/*c*.

Density considerations and the systematic weakness of all reflections with *k* + *l* odd placed the platinum atoms at the Wyckoff *a* sites (0, 0, 0) and (0, 1/2, 1/2). The remaining non-hydrogen atoms were located via successive structure factor—Fourier calculations using one atom from the first map to break the 2-fold degeneracy. Hydrogen atom positions were originally determined from difference maps for the water molecules and by calculation for the other three. Refinement proceeded so well that all hydrogen atoms were included. The complete least-squares full matrix, consisting of coordinates for all atoms except platinum, displacement parameters (isotropic for the hydrogen atoms, anisotropic otherwise), a secondary extinction coefficient (3.53×10^{-6}), and a scale factor, contained 188 variables. A final difference Fourier map showed deviations ranging from -1.32 to +1.42 e Å⁻³. All significant features are near the platinum and can be attributed to deficiencies in the absorption correction. The refinement converged with an *R* factor of 0.0250 (0.0209 for $F_o^2 > 3\sigma(F_o^2)$) and a goodness of fit of 1.96 for all 2874 reflections. Crystallographic data are given in Table I. The final parameters are listed in Table II.

Calculations were done with programs of the CRYM Crystallographic Computing System and ORTEP. Scattering factors and corrections for anomalous scattering were taken from a standard reference.⁶ $R = \sum |F_o| - |F_c| / \sum F_o$, for only $F_o^2 > 0$, and goodness of fit = $[\sum w(F_o^2 - F_c^2)^2 / (n - p)]^{1/2}$, where *n* is the number of data and *p* the number of parameters refined. The function minimized in least squares was $\sum w(F_o^2 - F_c^2)^2$, where $w = 1/\sigma^2(F_o^2)$. Variances of the individual reflections were assigned on the basis of counting statistics plus an additional term, 0.014-

**Figure 1.** ORTEP drawing of the dianion *trans*-[Pt(η²-dipic-*O,N*)₂]²⁻ with associated sodium cations and coordinated water molecules. Thermal ellipsoids are shown at the 80% probability level; hydrogen atoms are one-tenth scale.**Table III.** Selected Distances and Angles for Disodium *trans*-Bis(2,6-pyridinedicarboxylato-*O,N*)platinate(II) Hexahydrate^a

Distances (Å)			
Pt–N	2.016 (2)	C2–C3	1.378 (4)
Pt–O1	2.013 (2)	C3–C4	1.392 (4)
O1–C1	1.299 (3)	C4–C5	1.379 (4)
O2–C1	1.225 (3)	C5–C6	1.393 (3)
O3–C7	1.241 (3)	Na–O4	2.408 (2)
O4–C7	1.247 (3)	Na–O5	2.423 (3)
C1–C2	1.496 (3)	Na–O6	2.438 (2)
C7–C6	1.511 (3)	Na–O7	2.298 (3)
N–C2	1.355 (3)	Na–O6 _s	2.574 (2)
N–C6	1.347 (3)	Na–O2 _s	2.621 (2)

Angles (deg)			
O1–Pt–N	80.5 (0.7)	C3–C2–N	122.2 (2)
O1–Pt–N _s	99.5 (0.7)	C3–C2–C1	123.1 (2)
N–Pt–N _s	180	C4–C3–C2	118.3 (2)
O1–Pt–O1 _s	180	C5–C4–C3	119.1 (2)
Pt–O1–C1	114.3 (2)	C6–C5–C4	120.2 (2)
Pt–N–C2	111.6 (2)	C5–C6–N	120.1 (2)
Pt–N–C6	128.3 (2)	C7–C6–N	120.0 (2)
O2–C1–O1	123.8 (2)	C7–C6–C5	119.3 (2)
C2–C1–O1	114.6 (2)	O4–C7–O3	127.8 (2)
C2–C1–O2	121.5 (2)	C6–C7–O3	115.0 (2)
C6–N–C2	119.6 (2)	C6–C7–O4	117.1 (2)
C1–C2–N	114.6 (2)		

^a“s” denotes symmetry-related atom.

(*I*)². Variances of the merged reflections were determined by standard propagation of error plus another additional term, 0.014(*I*)². The absorption correction was done by Gaussian integration over an 8 × 8 grid. Transmission factors varied from 0.08 to 0.17.

Results and Discussion

We modified Zhou and Kostic's preparation² by using Na salts and higher concentrations and obtained direct precipitation of two types of crystals—microcrystalline purple needles and large, well-formed pale yellow cubes—after a few hours at room temperature. The first may contain partially oxidized, stacked [Pt(η³-dipic-*O,N,O*)Cl]⁻ anions as previously proposed;² we have not yet obtained crystals suitable for X-ray diffraction. The NMR spectrum of the yellow product was identical with that attributed² to *trans*-[Pt(η²-dipic-*N,O*)₂]²⁻; in particular, the appearance of three distinct aromatic proton signals establishes an asymmetric bonding mode for the chelating dipic ligand.

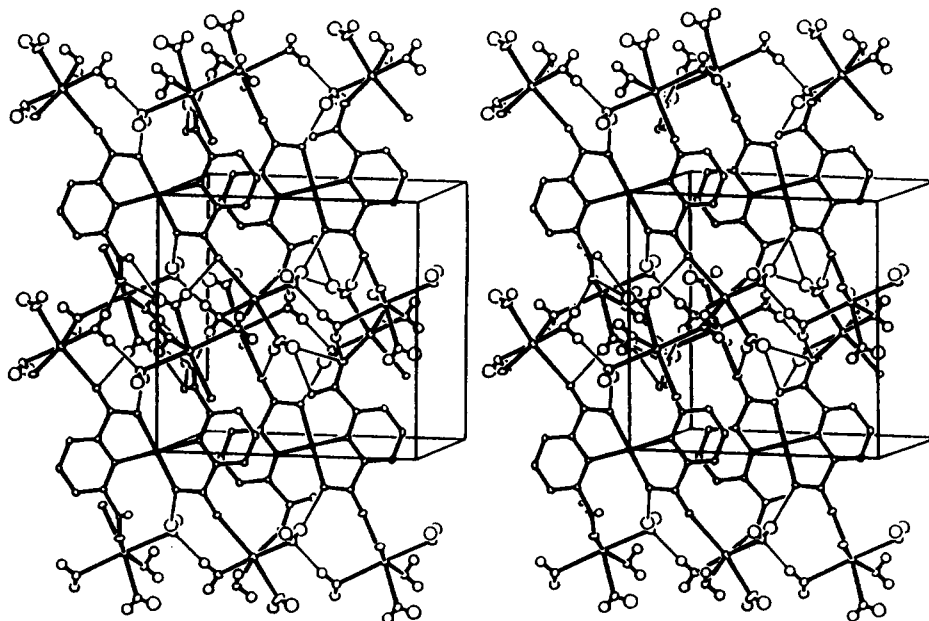
Coordination about Pt. The crystal structure verifies the previous proposal: two bidentate dipic-*O,N* ligands in a *trans* arrangement, giving a distorted square-planar coordination sphere (Figure 1). Deviations from the best plane defined by the platinum, coordinated CO₂, and pyridine ring atoms are as large as 0.27 Å, indicating a significant degree of “ruffling” imposed

(6) *International Tables for X-ray Crystallography*; Kynoch Press: Birmingham, England, 1974; Vol. IV, pp 71, 149.

Table IV. Comparison of Bonding Parameters (Å and deg) in dipic Complexes^a

complex	N-M	O1-M	C1-O1	C1-O2	N-M-O1	C1-N-M	C2-C1-N	O1-C2-C1	M-O1-C1	dihed ^b
[Pt(dipic) ₂] ²⁻	2.016	2.013	1.299	1.225	80.5	111.6	114.6	114.6	114.3	51.6
[Pt(dipic)Cl] ⁻	1.88-1.91	2.01-2.05	1.28-1.32	1.19-1.23	80.7-81.9	117.5-119.3 ^c	110-113	114-116	113.6-116	
Pt(pic)(dmsO)Cl ^d	2.032	1.994	1.285	1.232	80.6	112.7	114.8	116.7	115.0	
Ru(dipicH) ₂ Cl ₂	2.086	2.023	1.304	1.222	79.5	112.3	115.0	115.1	116.4	66.9 ^e
dipicH ₂ ^f			1.288-1.315	1.181-1.217			115.3-118.4	110.8-116.2		0.5-0.8

^a See Figure 1 for atom labels and see text for references. ^b Dihedral angle between the plane determined by the metal, coordinated carboxylate, and pyridine ring and the plane of the noncoordinated carboxylate. ^c Parameters not given in the original paper; recalculated from atom positions. ^d pic = 2-pyridinecarboxylate. ^e O1 is taken to be the protonated oxygen atom.

**Figure 2.** ORTEP stereoview of the crystal packing, with aromatic hydrogen atoms omitted and hydrogen bonds drawn in.

by chelate ring strain. Selected structural parameters are listed in Table III.

Comparisons of several key parameters with related species—the tridentate dipic-Pt complex,² a Pt complex of bidentate pyridine-2-carboxylate,⁷ the aforementioned Ru-dipicH complex,³ and free dipicH₂⁸—are given in Table IV. In all the complexes the intrachelate O-Pt-N angle (here 80.5 (7)°) is considerably below 90°, and the strained five-membered ring imposes additional constraints upon angles. For example, both M-N-C2 and N-C2-C1 are around 112-115° instead of the “natural” 120°; the only exception is M-N-C2 in [Pt(η³-dipic-O,N,O)Cl]⁻, which must be nearer 120° since both carboxylates are coordinated.

The difference between the coordinated (C1-O1) and noncoordinated (C1-O2) C=O bond lengths of the carboxylate group involved in bonding to Pt is pronounced, as is the case with the related complexes in Table IV, while C7-O3 and C7-O4 are nearly equal. (Note though that all these oxygens are involved in further interactions, either coordinated to Na or hydrogen bonded; see below.) The noncoordinated carboxylate group is twisted out of the pyridine/coordination plane, as is also the case for the previous η²-dipic structure (Table IV)³ but *not* for the free acid, where both carboxyl groups are essentially coplanar with the pyridine ring.⁸

Coordination about Na and Three-Dimensional Structure. The overall structure, shown in Figures 1 and 2, consists of alternating, interlinked layers of Pt complex anions and Na cations. Each Na is octahedrally coordinated, with two (cis) positions each occupied by an oxygen of the dipic carboxylate groups. One of these comes from a carboxylate that is *not* involved in bonding to Pt, while the other is the “free C=O” of a Pt-coordinated

carboxylate. The remaining four coordination sites are occupied by water molecules; of these, two bridge to adjacent sodium ions. The structure is further cross-linked by hydrogen bonding between all the hydrogen atoms and neighboring water or carboxylate oxygen centers. Presumably this extended structure is responsible for the facile crystallization of this hydrated sodium salt.

Acknowledgment. This research was supported by the Caltech Consortium in Chemistry and Chemical Engineering, founding members E. I. duPont de Nemours and Co., Inc., Eastman Kodak Co., Minnesota Mining and Manufacturing Co., and Shell Development Co. A.M.H. thanks the SERC (U.K.) for a NATO fellowship. We thank the NSF for a grant (CHE-8219039) in support of purchase of the diffractometer and Dr. W. P. Schaefer for valuable assistance.

Supplementary Material Available: Tables V-IX, listing crystal and intensity collection data, anisotropic displacement parameters, final hydrogen parameters, hydrogen bonds, and complete distances and angles (5 pages); Table X, listing observed and calculated structure factors (12 pages). Ordering information is given on any current masthead page.

Contribution from the 3M Corporate Research and Industrial and Electronic Sector Laboratories, St. Paul, Minnesota 55144

NMR Assignments of Alkylcyclopentadienyl Ligands in Zirconium and Platinum Complexes

Richard A. Newmark,* Larry D. Boardman, and Allen R. Siedle

Received July 26, 1990

Introduction

We have been investigating organometallic complexes of both zirconium and platinum containing alkyl-substituted cyclopentadienyl (Cp = η⁵-C₅H₅) ligands. Assignment of the protons

(7) Annibale, G.; Cattalini, L.; Canovese, L.; Pitteri, B.; Tiripicchio, A.; Tiripicchio Camellini, M.; Tobe, M. L. *J. Chem. Soc., Dalton Trans.* **1986**, 1101.

(8) Takusagawa, F.; Hirotsu, K.; Shimada, A. *Bull. Chem. Soc. Jpn.* **1973**, *46*, 2020.